AMERICAN ACADEMY® OF OPHTHALMOLOGY
The Eye M.D. Association

DRAFT CONSENSUS STATEMENT FOR COMMENT

September 14 2015

This statement was developed as a result of breakout group recommendations from the March 24, 2014 Developing Novel Endpoints for Premium IOLs Workshop held in Silver Spring, Maryland. The primary goal of the workshop was to improve the regulatory science for evaluating premium IOLs, which in turn may enhance the efficiency with which safe and effective premium IOLs get to the market.

We are indebted to the Task Force on Developing Novel Endpoints for Premium IOLs formed after the Workshop for developing these statements based on the workshop discussions and recommendations, available peer-reviewed scientific literature, and other expert opinions. The Task Force includes the following : Jack Holladay, MD, Chair; Adrian Glasser, PhD, Scott MacRae, MD, Samuel Masket, MD, and Walter Stark, MD. The FDA liaisons to this Task Force include the following: Malvina Eydelman, MD, Don Calogero, MS, Gene Hilmantel, OD, MS, Tieuvi Nguyen, PhD, RAC, Eva Rorer, MD, and Michelle Tarver, MD, PhD.

We would like to solicit broad input from industry and other interested parties.

Please send your comments, your affiliation and contact information with the title of the referenced document to hoskinscenter@aao.org by the following deadline: **November 10, 2015** Please note that comments received after close of the comment period will not be accepted.

DRAFT AMERICAN ACADEMY OF OPHTHALMOLOGY TASK FORCE CONSENSUS STATEMENT ON MEASUREMENT OF TILT, DECENTRATION, AND CHORD LENGTH MU

Definitions

- Decentration of an IOL is the lateral horizontal and vertical displacement of an IOL relative to the visual axis (Subject-Fixated Coaxially Sighted Corneal Light Reflex as described by Chang and Waring)
- Tilt of an IOL is the horizontal and vertical angle of an IOL relative to the visual axis (Subject-Fixated Coaxially Sighted Corneal Light Reflex as described by Chang and Waring)
- Chord Length Mu (μ)[11] should be measured also so that we know the centration relative to pupil center as well as visual axis. For some diffractive IOLs, the midpoint between pupil center and visual axis may be optimal. In either case, we know all parameters.

Tilt, Decentration, and Chord Length Mu

Tilt, Decentration and Chord Length Mu (μ) should be measured on all subjects with a premium IOL. Direct methods to measure IOL tilt are described below. In cases where an investigator believes that the tilt is having a clinically significant effect on a subject's vision, the induced astigmatism at the IOL plane should be calculated by taking into account the power of the implanted IOL and the tilt angle at the IOL plane (see Appendix B). Decentration greater than 1.0 mm is equivalent to 1.7° of apparent tilt.[2]

Direct Measures of Tilt and Decentration

1. Using Purkinje Images, effective lens position (ELP) and corneal curvature

The original description of measuring decentration and tilt using Purkinje images was by Phillips in 1988.[1] A method for measuring the tilt and decentration of intraocular lenses (IOLs) in the static eye using the Purkinje image locations is presented. The patient fixates on a target that is coaxial with the camera or is at a predetermined angle with the camera axis. A telecentric stop is introduced in the camera so the positions of the Purkinje images on the film are independent of their distance from the camera. Measurements of the image locations on the film are used with anterior chamber depth and corneal curvature measurement to calculate the tilt and decentration of the IOL. In a group of 14 randomly selected patients with posterior chamber IOLs, 13 gave Purkinje images that could be measured. The average tilt was 7.8 degrees and the average decentration was 0.7 mm.

Guyton simplified the method using a penlight in 1990[2], but sacrificed accuracy having the clinician estimate the distance between images. The apparent optical axis of an implanted intraocular lens (IOL) can be located by alignment of the examiner's hand light with the third and fourth Purkinje images from the front and back surfaces of the IOL. Tilt of the IOL can be estimated (or measured with an arc perimeter) by the angle between the apparent optical axis and the patient's line of sight (actual tilt approximately 0.85 x apparent tilt). Decentration of the IOL is easily detected, equal to the distance of the IOL optical axis from the center of the pupil. This simple technique can be used through the natural pupil with posterior chamber IOLs, providing the optical axis of the malpositioned IOL still passes through the pupil. There was no data provided in the article and the accuracy is not reported.
The Purkinje method has been substantiated many times over the past 20 years the most recent of which is by Nishi in 2010.[3] Acquisition of images in pseudophakic eyes with the Purkinje meter was simple and rapid. The method was highly reliable for 1 examiner and between 2 examiners.

Appendix A describes a modification to enhance the precision of the method proposed by Guyton.

2. Scheimpflug Imaging

Rosales in 2006 validated their Purkinje Imaging System[4] and in 2010 compared the Scheimpflug and Purkinje imaging.[5] The improved designs of intraocular lenses (IOLs) implanted during cataract surgery demand understanding of the possible effects of lens misalignment on optical performance. In this paper, they describe the implementation, set-up and validation of two methods to measure in vivo tilt and decentration of IOLs, one based on Purkinje imaging and the other on Scheimpflug imaging. The Purkinje system images the reflections of an oblique collimated light source on the anterior cornea and anterior and posterior IOL surfaces and relies on the well supported assumption of the linearity of the Purkinje images with respect to IOL tilt and decentration.

Scheimpflug imaging requires geometrical distortion correction and image processing techniques to retrieve the pupillary axis, IOL axis and pupil center from the three-dimensional anterior segment image of the eye. Validation of the techniques using a physical eye model indicates that IOL tilt is estimated within an accuracy of 0.261 degree and decentration within 0.161 mm. Measurements on patients implanted with aspheric IOLs indicate that IOL tilt and decentration tend to be mirror symmetric between left and right eyes. The average tilt was 1.54 degrees and the average decentration was 0.21 mm. Simulated aberration patterns using custom models of the patients' eyes, built using anatomical data of the anterior cornea and foveal position, the IOL geometry and the measured IOL tilt and decentration predict the experimental wave aberrations measured using laser ray tracing aberrometry on the same eyes. This reveals a relatively minor contribution of IOL tilt and decentration on the higher-order aberrations of the normal pseudophakic eye.

<u>Indirect Measure of Tilt at the IOL Plane</u>

The vector difference between the NET CORNEAL ASTIGMATISM (front and back corneal surface) and the Refractive Astigmatism at the corneal plane is the lenticular (phakic or pseudophakic) astigmatism at the corneal plane. In mathematical form:

Net Corneal Astigmatism + Lenticular Astigmatism = Refractive Astigmatism

or

Lenticular Astigmatism = Refractive Astigmatism - Net Corneal Astigmatism

Since the ***Refractive Astigmatism*** of an eye has the opposite sign of the ***Refractive Error Astigmatism*** of the eye, the equation can be written:

Lenticular Astigmatism = -Refractive Error Astigmatism - Net Corneal Astigmatism

The equation above describes the lenticular astigmatism at the corneal plane. If the vector differences are not oblique, the method for oblique cylinders between the keratometric and refractive error astigmatism is identical and completely described in Reference 6.
If Net Corneal Astigmatism or Equivalent K-reading astigmatism[7] are not available, and only anterior surface K-readings are available, then the anterior surface K-reading may be modified to Net Corneal Power by adding 0.22 D @ 180° (against-the-rule) vector to the anterior K-reading vector.[8,9] This would

reduce with-the-rule by 0.22 D, increase against-the-rule by 0.22 D and oblique astigmatism somewhere between, depending on the axis. According to the data in the two references, the resulting Net Corneal power will be within 0.25 D of the correct power 90% of the time.

The lenticular astigmatism needs to be converted from the corneal plane to the IOL plane. The conversion depends on the Effective Lens Position and the power of the IOL. The exact conversion ratio can be determined postoperatively by using the Spheroequivalent Refraction, K-reading, axial length and IOL power to calculate the actual ELP for a specific patient using Equations 13a-f on page 1367 in Reference 10. Using the actual ELP and the actual IOL Power, the exact ratio may be interpolated from the Table 1 below or calculated using the vergence formula (Equation 2 page 1359) in reference 10.

Table 1

	Effective Lens Position (ELP)					
A-constant—>	116.346	117.203	118.059	**118.916**	119.773	120.630
Surgeon Factor—>	0.287	0.772	1.257	**1.742**	2.227	2.713
ELP—>	**4.000**	**4.500**	**5.000**	**5.500**	**6.000**	**6.500**
IOL POWER	***Resulting Ratio of IOL Toricity to 2 D of Corneal Astigmatism***					
10	1.359	1.424	1.494	1.571	1.654	1.745
22	1.277	1.330	1.387	1.450	1.519	1.595
34	1.198	1.239	1.284	1.334	1.390	1.452
46	1.121	1.151	1.185	1.223	1.267	1.316

Finally, the lenticular astigmatism at the IOL plane is used in the Table in Appendix B along with the IOL power, to estimate the tilt angle of the IOL.

Appendix A - Quantification of the Guyton Method

<u>Background</u>

The Guyton method[1] is a simple, rapid and accurate procedure for determining the tilt of an IOL **when the IOL is decentered less than 1 mm** (1mm produces 1.7° of apparent tilt and 2 mm 4.14° of apparent tilt). The procedure suggests the use of an arc scan perimeter which is unavailable to most practitioners at this time. The following procedure for taking measurements is recommended so that the angular tilt of an IOL in the absence of significant decentration may be determined.

<u>Standard Operating Procedure</u>

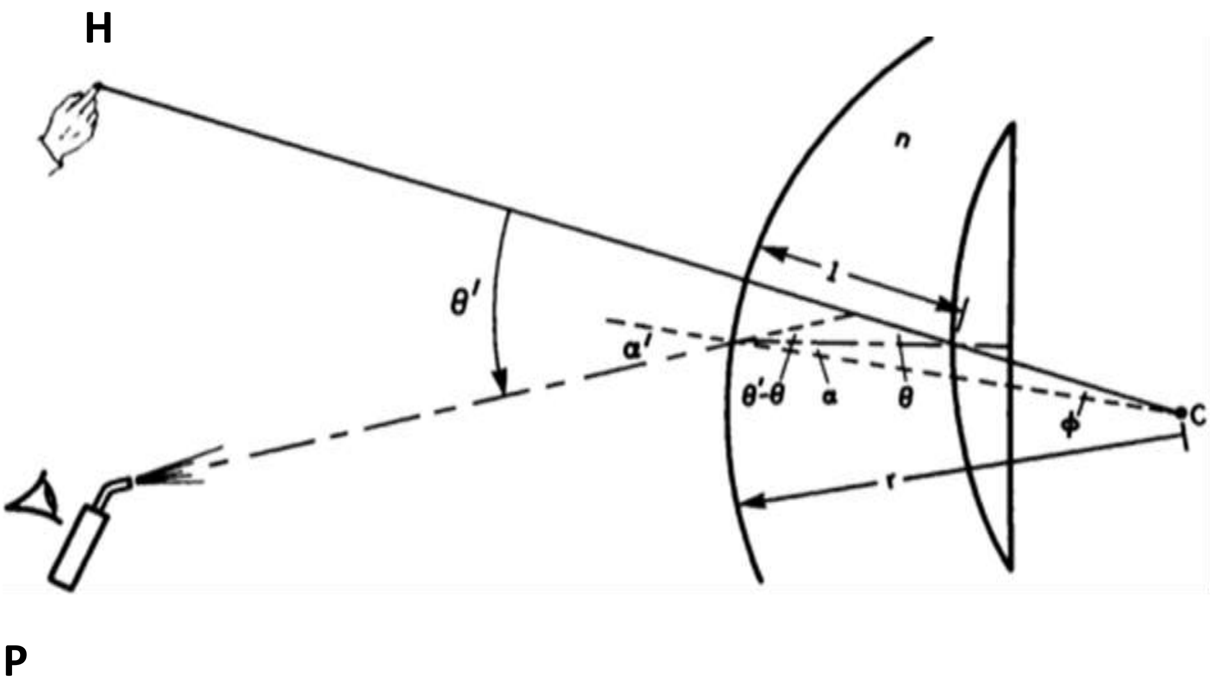

(Figure 8 modified from Guyton). The IOL is tilted about its anterior vertex of the IOL and not decentered. The actual tilt (θ) can be shown in this case to be equal to approximately 0.85 times the apparent tilt (0.85 θ'). [For values from the Gullstrand schematic eye: **n = 1.336, l = 3.6 mm, and r = 7.70 mm, θ = 0.85 θ'**]

The triangle forming angle θ' is formed by point **V** (vertex), point **P** (penlight) and point **H** (hand). Point V is about one-half of the depth of the anterior vertex of the IOL from the anterior vertex of the cornea and is ~ 4.5 mm for modern day posterior chamber IOLs in-the-bag, so would be ~ 2.2 mm. Since this distance is negligible relative to distances **VP** (nominally ~ 65 cm) and **VH** (nominally ~ 65 cm) it can be ignored. By measuring the distances **VP**, **VH** and **PH** angle **θ** may be determined.

From the Law of Cosines

$$HP^2 = VP^2 + VH^2 - 2\,VP\,VH\,\cos\theta'$$
$$\theta' = \cos^{-1}\left[\frac{VP^2 + VH^2 - HP^2}{2\,VP\;VH}\right]$$
$$\theta = 0.85\,\theta'$$

Example:

For VP = 65 cm, VH = 65 cm and HP = 10 cm

$$\theta' = \cos^{-1}\left[\frac{65^2 + 65^2 - 10^2}{2 \cdot 65 \cdot 65}\right]$$
$$\theta' = \cos^{-1}\left[\frac{8350}{8450}\right]$$
$$\theta' = 8.8235°$$
$$\theta = 7.4999°$$

The **direction of tilt** as mentioned by Davis, is the angle of the plane through the visual axis (PV in Figure 8 above) and is the same as the semi-meridians of the cornea (0° is left ear, 90° is superior, 180° is right ear and 270° is inferior).

DECENTRATION MEASUREMENT:

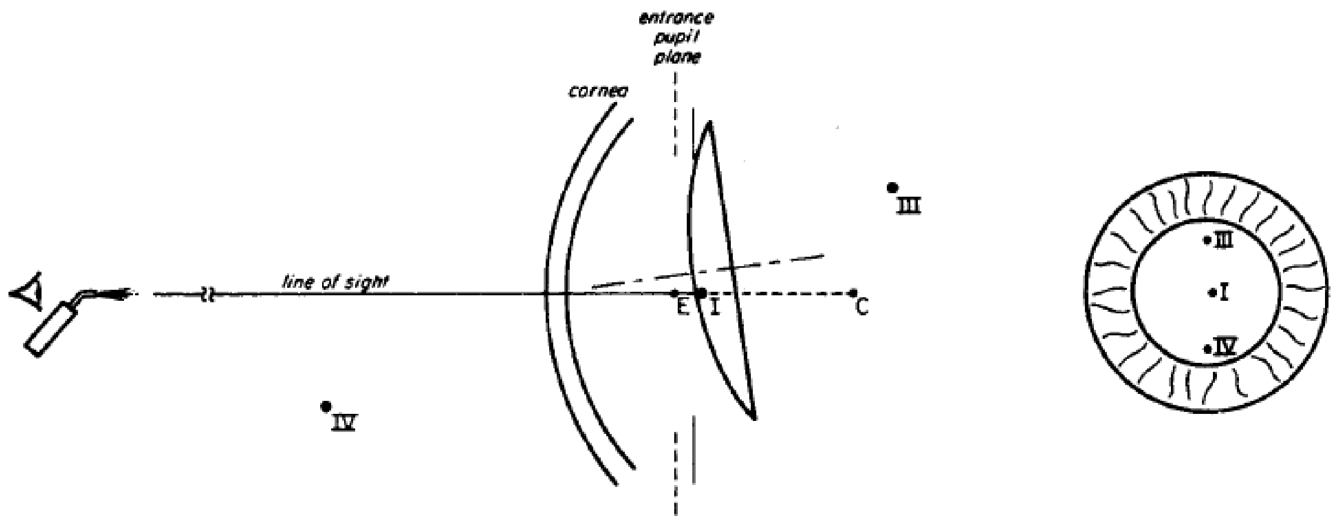

Figure 5. Forward tilt and upward decentration of a forward-optic IOL (in this case convex-plano, but also is the same for a biconvex). The patient's line of sight passes from the center of the entrance pupil (E) to the fixation object (the hand light in this illustration). Purkinje images III and IV are displaced in opposite directions from the line of sight. Notice that the line connecting images III and IV is tilted approximately twice as much as the optical axis of the IOL, thus magnifying the apparent tilt of the IOL.

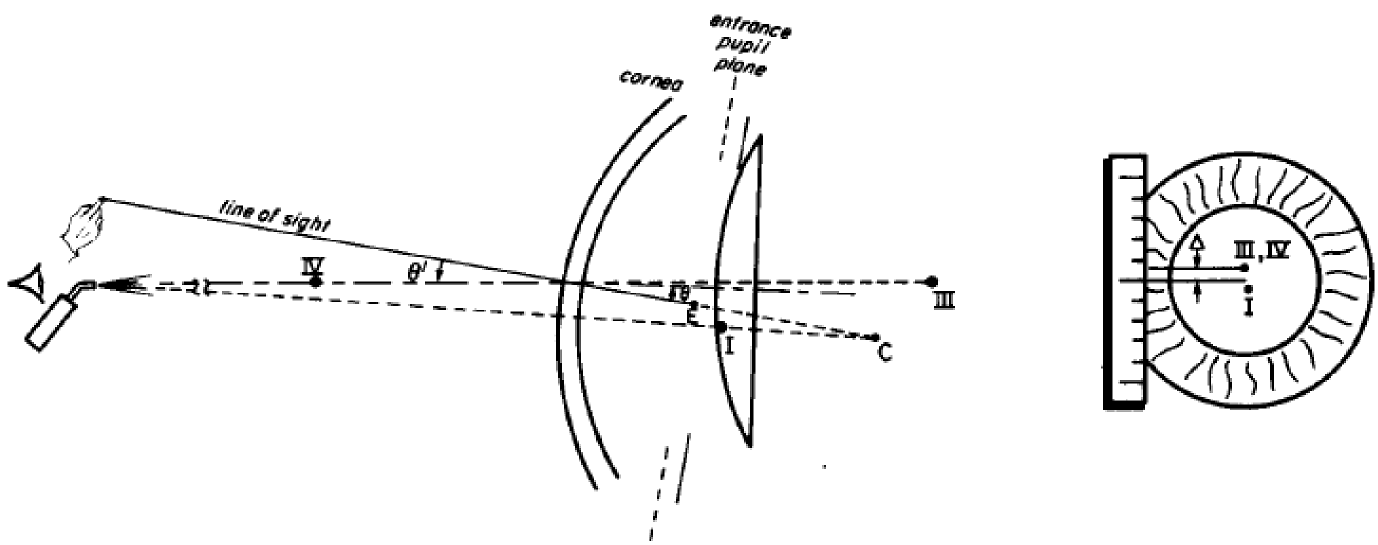

Figure 6. With the patient looking at the examiner's finger, the examiner moves his finger in the frontal plane until Purkinje images III and IV, as sighted by the examiner's eye, become aligned with one another. The apparent IOL tilt (θ') and decentration (Δ) are directly determined from this viewing situation.

In this example, the Purkinje images III and IV when superimposed are superior (90°) to Purkinje I and represent upward decentration. **The decentration may have a vertical and horizontal component such that the total decentration is the square root of the sum of the squares of the two components.**

Note: The Direction of Tilt may be from 0° to 359° for measuring θ'. The meridian about which the IOL is tilted is 90° from the Direction of Tilt and in the example above (Figure 6) is the 0° or 180° meridian or the horizontal. Also, the decentration is measured relative to Purkinje 1 (vertex normal and near visual axis), not the center of the pupil. An IOL will be considered perfectly centered when Purkinje I, III and IV are superimposable. This IOL will appear nasal (0.33 mm and slightly inferior) relative to the pupil center (angle Kappa or Lambda) or Chord Length Distance (μ) as defined by Chang and Waring[11]

A Simple Device for Quantitative Phaco-angulometry

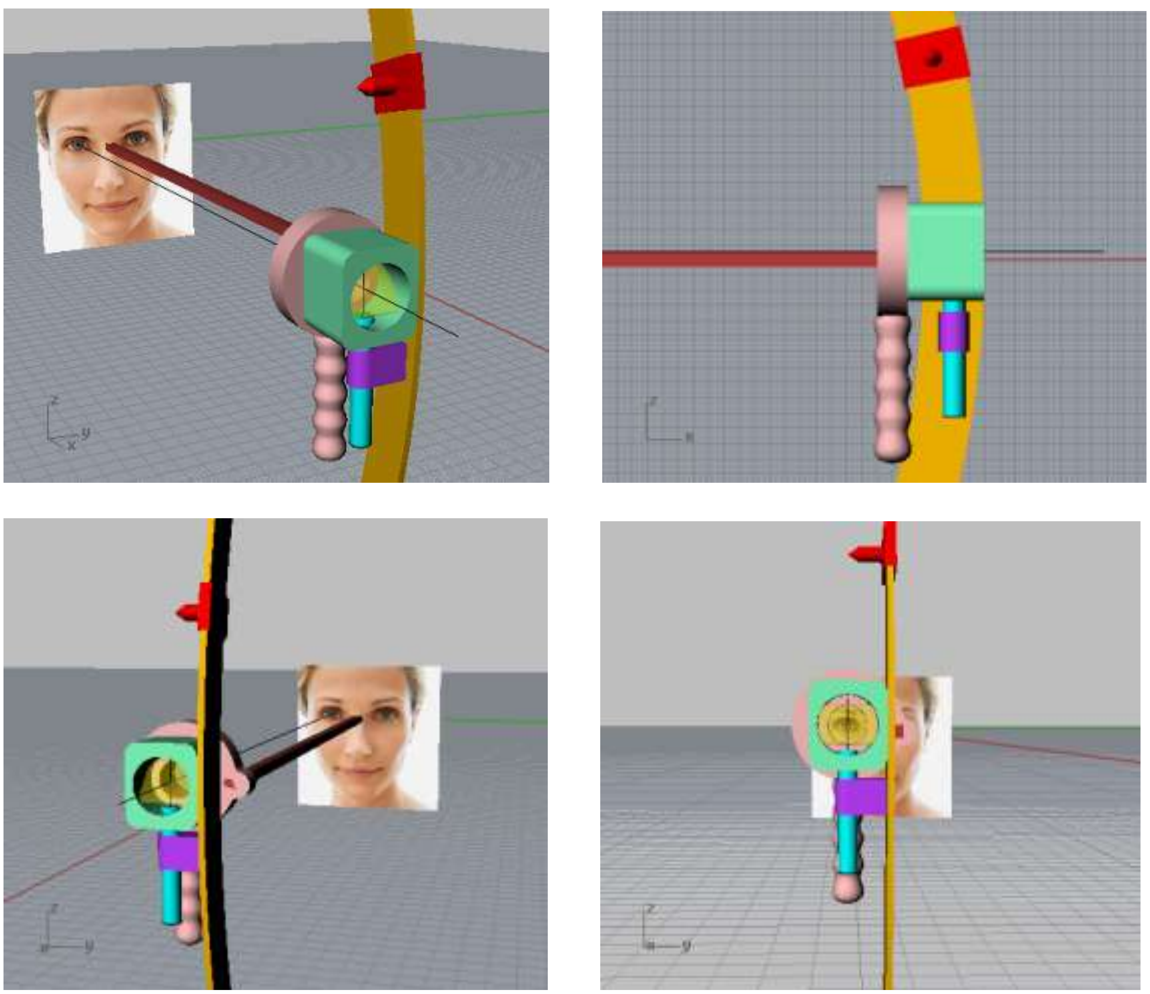

The images show the design of a simple, low cost device that could be used for phaco-angulometry. It consists of a handle (pink) with a hole through which the patient's eye can be viewed by the examiner. To the handle is mounted a rotating cube (green) with a hole that houses a 45-degree angled beam splitter within, a pen-light below (blue) and an arc (gold) to the side. Light from the pen-light shines up and is reflected from the beam-splitter into the patient's eye. A sliding fixation target (red) is affixed to the arc. The center of curvature of the arc is at the vertex of the cornea. The arc is etched with degree markings. To the side of the handle is attached a light balsawood square dowel rod that is touched to the bridge of the patient's nose to fix the working distance. With the patient looking at the fixation target, the examiner moves the fixation target along the arc and rotates the cube and arc until Purkinje images III and IV, as sighted by the examiner's eye, become aligned with one another.

References

[1] Phillips P, Pérez-Emmanuelli J, Rosskothen HD, Koester CJ. Measurement of intraocular lens decentration and tilt in vivo. J Cataract Refract Surg. 1988 Mar;14(2):129-35.
[2] Guyton DL, Uozato H, Wisnicki HJ. Rapid determination of intraocular lens tilt and decentration through the undilated pupil. Ophthalmology. 1990 Oct;97(10):1259-64.
[3] Nishi Y1, Hirnschall N, Crnej A, Gangwani V, Tabernero J, Artal P, Findl O. Reproducibility of intraocular lens decentration and tilt measurement using a clinical Purkinje meter. J Cataract Refract Surg. 2010 Sep;36(9):1529-35.
[4] Rosales P, Marcos S. Phakometry and lens tilt and decentration using a custom-developed Purkinje imaging apparatus: Validation and measurements. j Opt Soc Am A. 2006;23:509-520.
[5] Rosales P, De Castro A, Jiménez-Alfaro I, Marcos S. Intraocular lens alignment from purkinje and Scheimpflug imaging. Clin Exp Optom. 2010 Nov;93(6):400-8.
[6] Holladay JT, Cravy TV, Koch DD. Calculating the surgically induced refractive change following ocular surgery. J Cataract Refract Surg. 1992; 18: 429-43.
[7] Holladay JT, Hill WE, Steinmueller A: Corneal Power Measurements Using Scheimpflug Imaging in Eyes With Prior Corneal Refractive Surgery. J Refract Surg. 2009;25:862-868.
[8] Koch DD, Ali SF, Weikert MP, Shirayama M, Jenkins R, Wang L. Contribution of posterior corneal astigmatism to total corneal astigmatism. J Cataract Refract Surg 2012; 38:2080–2087.
[9] Savini G, Versaci F, Vestri G, Ducoli P, Naeser K. Influence of posterior corneal astigmatism on total corneal astigmatism in eyes with moderate to high astigmatism. J Cataract Refract Surg 2014; 40:1645–1653.
[10] Holladay JT. Standardizing constants for ultrasonic biometry, keratometry, and intraocular lens power calculations. J Cataract Refract Surg. 1997; 23: 1356-70.
[11] Chang DH, Waring IV GO. The Subject-Fixated Coaxially Sighted Corneal Light Reflex: A Clinical Marker for Centration of Refractive Treatments and Devices. Am J Ophthalmol 2014;158:863–874.

AppendixB

INDUCED ASTIGMATISM (D) for TILT ANGLE (Degrees) versus IOL POWER (D) • **VALUES > 2.0 D shaded in RED**

TILT ANGLE α (Degrees)	IOL Power (D) 1	2	3	4	5	6	7	8	9	10	11	12	13	14	15	16	17	18	19	20
1	0.00	0.00	0.00	0.00	0.00	0.00	0.00	0.00	0.00	0.00	0.00	0.00	0.00	0.00	0.00	0.00	0.01	0.01	0.01	0.01
2	0.00	0.00	0.00	0.00	0.01	0.01	0.01	0.01	0.01	0.01	0.01	0.01	0.02	0.02	0.02	0.02	0.02	0.02	0.02	0.02
3	0.00	0.01	0.01	0.01	0.01	0.02	0.02	0.02	0.02	0.03	0.03	0.03	0.04	0.04	0.04	0.04	0.05	0.05	0.05	0.05
4	0.00	0.01	0.01	0.02	0.02	0.03	0.03	0.04	0.04	0.05	0.05	0.06	0.06	0.07	0.07	0.08	0.08	0.09	0.09	0.10
5	0.01	0.02	0.02	0.03	0.04	0.05	0.05	0.06	0.07	0.08	0.08	0.09	0.10	0.11	0.12	0.12	0.13	0.14	0.15	0.15
6	0.01	0.02	0.03	0.04	0.05	0.07	0.08	0.09	0.10	0.11	0.12	0.13	0.14	0.15	0.17	0.18	0.19	0.20	0.21	0.22
7	0.02	0.03	0.05	0.06	0.08	0.09	0.11	0.12	0.14	0.15	0.17	0.18	0.20	0.21	0.23	0.24	0.26	0.27	0.29	0.30
8	0.02	0.04	0.06	0.08	0.10	0.12	0.14	0.16	0.18	0.20	0.22	0.24	0.26	0.28	0.30	0.32	0.34	0.36	0.38	0.40
9	0.03	0.05	0.08	0.10	0.13	0.15	0.18	0.20	0.23	0.25	0.28	0.30	0.33	0.35	0.38	0.40	0.43	0.46	0.48	0.51
10	0.03	0.06	0.09	0.13	0.16	0.19	0.22	0.25	0.28	0.31	0.35	0.38	0.41	0.44	0.47	0.50	0.53	0.57	0.60	0.63
11	0.04	0.08	0.11	0.15	0.19	0.23	0.27	0.31	0.34	0.38	0.42	0.46	0.50	0.54	0.57	0.61	0.65	0.69	0.73	0.76
12	0.05	0.09	0.14	0.18	0.23	0.27	0.32	0.37	0.41	0.46	0.50	0.55	0.60	0.64	0.69	0.73	0.78	0.82	0.87	0.92
13	0.05	0.11	0.16	0.22	0.27	0.33	0.38	0.43	0.49	0.54	0.60	0.65	0.70	0.76	0.81	0.87	0.92	0.98	1.03	1.09
14	0.06	0.13	0.19	0.25	0.32	0.38	0.44	0.51	0.57	0.63	0.70	0.76	0.82	0.88	0.95	1.01	1.08	1.14	1.20	1.27
15	0.07	0.15	0.22	0.29	0.37	0.44	0.51	0.59	0.66	0.73	0.81	0.88	0.95	1.03	1.10	1.17	1.25	1.32	1.39	1.47
16	0.08	0.17	0.25	0.34	0.42	0.51	0.59	0.67	0.76	0.84	0.93	1.01	1.10	1.18	1.26	1.35	1.43	1.52	1.60	1.69
17	0.10	0.19	0.29	0.38	0.48	0.58	0.67	0.77	0.87	0.96	1.06	1.15	1.25	1.35	1.44	1.54	1.63	1.73	1.83	1.92
18	0.11	0.22	0.33	0.44	0.54	0.65	0.76	0.87	0.98	1.09	1.20	1.31	1.42	1.53	1.63	1.74	1.85	1.96	2.07	2.18
19	0.12	0.25	0.37	0.49	0.61	0.74	0.86	0.98	1.10	1.23	1.35	1.47	1.60	1.72	1.84	1.96	2.09	2.21	2.33	2.45
20	0.14	0.28	0.41	0.55	0.69	0.83	0.96	1.10	1.24	1.38	1.51	1.65	1.79	1.93	2.06	2.20	2.34	2.48	2.62	2.75
21	0.15	0.31	0.46	0.61	0.77	0.92	1.08	1.23	1.38	1.54	1.69	1.84	2.00	2.15	2.30	2.46	2.61	2.77	2.92	3.07
22	0.17	0.34	0.51	0.68	0.85	1.03	1.20	1.37	1.54	1.71	1.88	2.05	2.22	2.39	2.56	2.73	2.90	3.08	3.25	3.42
23	0.19	0.38	0.57	0.76	0.95	1.14	1.33	1.51	1.70	1.89	2.08	2.27	2.46	2.65	2.84	3.03	3.22	3.41	3.60	3.79
24	0.21	0.42	0.63	0.84	1.05	1.25	1.46	1.67	1.88	2.09	2.30	2.51	2.72	2.93	3.14	3.35	3.56	3.76	3.97	4.18
25	0.23	0.46	0.69	0.92	1.15	1.38	1.61	1.84	2.07	2.30	2.53	2.76	3.00	3.23	3.46	3.69	3.92	4.15	4.38	4.61
26	0.25	0.51	0.76	1.01	1.27	1.52	1.77	2.02	2.28	2.53	2.78	3.04	3.29	3.54	3.80	4.05	4.30	4.56	4.81	5.06
27	0.28	0.55	0.83	1.11	1.39	1.66	1.94	2.22	2.50	2.77	3.05	3.33	3.61	3.88	4.16	4.44	4.72	4.99	5.27	5.55
28	0.30	0.61	0.91	1.21	1.52	1.82	2.12	2.43	2.73	3.03	3.34	3.64	3.95	4.25	4.55	4.86	5.16	5.46	5.77	6.07
29	0.33	0.66	0.99	1.32	1.66	1.99	2.32	2.65	2.98	3.31	3.64	3.97	4.31	4.64	4.97	5.30	5.63	5.96	6.29	6.63
30	0.36	0.72	1.08	1.44	1.81	2.17	2.53	2.89	3.25	3.61	3.97	4.33	4.69	5.05	5.42	5.78	6.14	6.50	6.86	7.22
31	0.39	0.79	1.18	1.57	1.96	2.36	2.75	3.14	3.54	3.93	4.32	4.72	5.11	5.50	5.89	6.29	6.68	7.07	7.47	7.86
32	0.43	0.85	1.28	1.71	2.14	2.56	2.99	3.42	3.84	4.27	4.70	5.12	5.55	5.98	6.41	6.83	7.26	7.69	8.11	8.54
33	0.46	0.93	1.39	1.85	2.32	2.78	3.24	3.71	4.17	4.63	5.10	5.56	6.02	6.49	6.95	7.41	7.88	8.34	8.81	9.27
34	0.50	1.00	1.51	2.01	2.51	3.01	3.52	4.02	4.52	5.02	5.53	6.03	6.53	7.03	7.54	8.04	8.54	9.04	9.55	10.05
35	0.54	1.09	1.63	2.18	2.72	3.26	3.81	4.35	4.90	5.44	5.98	6.53	7.07	7.62	8.16	8.70	9.25	9.79	10.34	10.88
36	0.59	1.18	1.77	2.36	2.94	3.53	4.12	4.71	5.30	5.89	6.48	7.06	7.65	8.24	8.83	9.42	10.01	10.60	11.19	11.77
37	0.64	1.27	1.91	2.55	3.19	3.82	4.46	5.09	5.73	6.37	7.00	7.64	8.27	8.91	9.55	10.19	10.82	11.46	12.09	12.73
38	0.69	1.38	2.06	2.75	3.44	4.13	4.81	5.50	6.19	6.88	7.56	8.25	8.94	9.63	10.31	11.00	11.69	12.38	13.06	13.75
39	0.74	1.49	2.23	2.97	3.71	4.46	5.20	5.94	6.69	7.42	8.17	8.91	9.65	10.39	11.15	11.89	12.63	13.37	14.11	14.85
40	0.80	1.60	2.40	3.20	4.01	4.81	5.61	6.41	7.21	8.01	8.81	9.61	10.41	11.21	12.02	12.82	13.62	14.42	15.22	16.02
41	0.86	1.73	2.59	3.46	4.32	5.18	6.05	6.91	7.78	8.64	9.50	10.37	11.23	12.10	12.96	13.83	14.69	15.55	16.42	17.28
42	0.93	1.86	2.80	3.73	4.66	5.59	6.52	7.46	8.39	9.32	10.25	11.18	12.11	13.04	13.98	14.91	15.84	16.77	17.70	18.63
43	1.00	2.01	3.01	4.02	5.02	6.03	7.03	8.04	9.04	10.04	11.05	12.05	13.06	14.06	15.07	16.07	17.07	18.08	19.08	20.09
44	1.08	2.17	3.25	4.33	5.41	6.50	7.58	8.66	9.74	10.83	11.91	12.99	14.07	15.16	16.24	17.32	18.40	19.49	20.57	21.65
45	1.17	2.33	3.50	4.67	5.83	7.00	8.17	9.33	10.50	11.67	12.83	14.00	15.17	16.33	17.50	18.67	19.83	21.00	22.17	23.33
46	1.26	2.51	3.77	5.03	6.28	7.54	8.80	10.06	11.31	12.57	13.83	15.09	16.34	17.60	18.86	20.12	21.37	22.63	23.89	25.15
47	1.36	2.71	4.07	5.42	6.78	8.13	9.49	10.84	12.20	13.56	14.91	16.27	17.62	18.97	20.33	21.69	23.04	24.39	25.75	27.10
48	1.46	2.92	4.38	5.84	7.30	8.76	10.22	11.68	13.14	14.61	16.07	17.53	18.99	20.45	21.91	23.37	24.83	26.29	27.75	29.21
49	1.57	3.15	4.72	6.30	7.87	9.45	11.02	12.60	14.17	15.75	17.32	18.90	20.47	22.04	23.62	25.19	26.77	28.34	29.92	31.49
50	1.70	3.40	5.09	6.79	8.49	10.19	11.89	13.58	15.28	16.98	18.68	20.38	22.08	23.77	25.47	27.17	28.87	30.57	32.26	33.96
51	1.83	3.66	5.50	7.33	9.16	10.99	12.82	14.66	16.49	18.32	20.15	21.98	23.82	25.65	27.48	29.31	31.14	32.98	34.81	36.64
52	1.98	3.95	5.93	7.91	9.89	11.86	13.84	15.82	17.80	19.77	21.75	23.73	25.71	27.68	29.66	31.64	33.61	35.59	37.57	39.55
53	2.14	4.27	6.41	8.54	10.68	12.81	14.95	17.08	19.22	21.36	23.49	25.63	27.76	29.90	32.03	34.17	36.30	38.44	40.57	42.71
54	2.31	4.62	6.92	9.23	11.54	13.85	16.15	18.46	20.77	23.08	25.38	27.69	30.00	32.31	34.62	36.92	39.23	41.54	43.85	46.15
55	2.50	4.99	7.49	9.98	12.48	14.97	17.47	19.97	22.46	24.96	27.45	29.95	32.45	34.94	37.44	39.93	42.43	44.92	47.42	49.92
56	2.70	5.40	8.10	10.81	13.51	16.21	18.91	21.61	24.31	27.02	29.72	32.42	35.12	37.82	40.52	43.22	45.93	48.63	51.33	54.03
57	2.93	5.85	8.78	11.71	14.64	17.56	20.49	23.42	26.34	29.27	32.20	35.13	38.05	40.98	43.91	46.83	49.76	52.69	55.62	58.54
58	3.18	6.35	9.53	12.70	15.88	19.05	22.23	25.40	28.58	31.75	34.93	38.10	41.28	44.45	47.63	50.80	53.98	57.15	60.33	63.50
59	3.45	6.90	10.34	13.79	17.24	20.69	24.14	27.59	31.03	34.48	37.93	41.38	44.83	48.27	51.72	55.17	58.62	62.07	65.52	68.96
60	3.75	7.50	11.25	15.00	18.75	22.50	26.25	30.00	33.75	37.50	41.25	45.00	48.75	52.50	56.25	60.00	63.75	67.50	71.25	75.00

TILT ANGLE α (Degrees)	21	22	23	24	25	26	27	28	29	30	31	32	33	34	35	36	37	38	39	40
1	0.01	0.01	0.01	0.01	0.01	0.01	0.01	0.01	0.01	0.01	0.01	0.01	0.01	0.01	0.01	0.01	0.01	0.01	0.01	0.01
2	0.03	0.03	0.03	0.03	0.03	0.03	0.03	0.03	0.04	0.04	0.04	0.04	0.04	0.04	0.04	0.04	0.05	0.05	0.05	0.05
3	0.06	0.06	0.06	0.07	0.07	0.07	0.07	0.08	0.08	0.08	0.08	0.09	0.09	0.09	0.10	0.10	0.10	0.10	0.11	0.11
4	0.10	0.11	0.11	0.12	0.12	0.13	0.13	0.14	0.14	0.15	0.15	0.16	0.16	0.17	0.17	0.18	0.18	0.18	0.19	0.20
5	0.16	0.17	0.18	0.19	0.19	0.20	0.21	0.21	0.22	0.23	0.24	0.25	0.25	0.26	0.27	0.28	0.28	0.29	0.30	0.31
6	0.23	0.24	0.26	0.27	0.28	0.29	0.30	0.31	0.32	0.33	0.34	0.35	0.37	0.38	0.39	0.40	0.41	0.42	0.43	0.44
7	0.32	0.33	0.35	0.36	0.38	0.39	0.41	0.42	0.44	0.45	0.47	0.48	0.50	0.52	0.53	0.55	0.56	0.58	0.59	0.61
8	0.42	0.44	0.46	0.48	0.50	0.52	0.54	0.56	0.58	0.60	0.62	0.64	0.66	0.68	0.70	0.72	0.74	0.76	0.78	0.80
9	0.53	0.56	0.58	0.61	0.63	0.66	0.68	0.71	0.73	0.76	0.78	0.81	0.83	0.86	0.88	0.91	0.94	0.96	0.99	1.01
10	0.66	0.69	0.72	0.75	0.79	0.82	0.85	0.88	0.91	0.94	0.97	1.00	1.04	1.07	1.10	1.13	1.16	1.19	1.22	1.26
11	0.80	0.84	0.88	0.92	0.96	0.99	1.03	1.07	1.11	1.15	1.19	1.22	1.26	1.30	1.34	1.38	1.41	1.45	1.49	1.53
12	0.96	1.01	1.05	1.10	1.15	1.19	1.24	1.28	1.33	1.37	1.42	1.47	1.51	1.56	1.60	1.65	1.70	1.74	1.79	1.83
13	1.14	1.19	1.25	1.30	1.35	1.41	1.46	1.52	1.57	1.63	1.68	1.73	1.79	1.84	1.90	1.95	2.01	2.06	2.11	2.17
14	1.33	1.39	1.46	1.52	1.58	1.65	1.71	1.77	1.84	1.90	1.96	2.03	2.09	2.15	2.22	2.28	2.34	2.41	2.47	2.54
15	1.54	1.61	1.69	1.76	1.83	1.91	1.98	2.06	2.13	2.20	2.28	2.35	2.42	2.50	2.57	2.64	2.72	2.79	2.86	2.94
16	1.77	1.85	1.94	2.02	2.11	2.19	2.28	2.36	2.44	2.53	2.61	2.70	2.78	2.87	2.95	3.03	3.12	3.20	3.29	3.37
17	2.02	2.11	2.21	2.31	2.40	2.50	2.60	2.69	2.79	2.88	2.98	3.08	3.17	3.27	3.36	3.46	3.56	3.65	3.75	3.85
18	2.29	2.40	2.51	2.61	2.72	2.83	2.94	3.05	3.16	3.27	3.38	3.49	3.59	3.70	3.81	3.92	4.03	4.14	4.25	4.36
19	2.58	2.70	2.82	2.95	3.07	3.19	3.31	3.44	3.56	3.68	3.81	3.93	4.05	4.17	4.30	4.42	4.54	4.66	4.79	4.91
20	2.89	3.03	3.17	3.30	3.44	3.58	3.72	3.85	3.99	4.13	4.27	4.40	4.54	4.68	4.82	4.96	5.09	5.23	5.37	5.51
21	3.23	3.38	3.53	3.69	3.84	4.00	4.15	4.30	4.46	4.61	4.76	4.92	5.07	5.22	5.38	5.53	5.69	5.84	5.99	6.15
22	3.59	3.76	3.93	4.10	4.27	4.44	4.61	4.78	4.95	5.13	5.30	5.47	5.64	5.81	5.98	6.15	6.32	6.49	6.66	6.83
23	3.98	4.17	4.36	4.54	4.73	4.92	5.11	5.30	5.49	5.68	5.87	6.06	6.25	6.44	6.63	6.82	7.01	7.20	7.38	7.57
24	4.39	4.60	4.81	5.02	5.23	5.44	5.65	5.86	6.07	6.27	6.48	6.69	6.90	7.11	7.32	7.53	7.74	7.95	8.16	8.37
25	4.84	5.07	5.30	5.53	5.76	5.99	6.22	6.45	6.68	6.91	7.14	7.37	7.60	7.83	8.06	8.29	8.52	8.75	8.99	9.22
26	5.32	5.57	5.82	6.07	6.33	6.58	6.83	7.09	7.34	7.59	7.85	8.10	8.35	8.61	8.86	9.11	9.37	9.62	9.87	10.12
27	5.83	6.10	6.38	6.66	6.94	7.21	7.49	7.77	8.05	8.32	8.60	8.88	9.16	9.43	9.71	9.99	10.27	10.54	10.82	11.10
28	6.37	6.68	6.98	7.28	7.59	7.89	8.19	8.50	8.80	9.10	9.41	9.71	10.02	10.32	10.62	10.93	11.23	11.53	11.84	12.14
29	6.96	7.29	7.62	7.95	8.28	8.61	8.94	9.28	9.61	9.94	10.27	10.60	10.93	11.27	11.60	11.93	12.26	12.59	12.92	13.25
30	7.58	7.94	8.31	8.67	9.03	9.39	9.75	10.11	10.47	10.83	11.19	11.56	11.92	12.28	12.64	13.00	13.36	13.72	14.08	14.44
31	8.25	8.65	9.04	9.43	9.82	10.22	10.61	11.00	11.40	11.79	12.18	12.57	12.97	13.36	13.75	14.15	14.54	14.93	15.33	15.72
32	8.97	9.39	9.82	10.25	10.68	11.10	11.53	11.96	12.38	12.81	13.24	13.66	14.09	14.52	14.95	15.37	15.80	16.23	16.65	17.08
33	9.73	10.20	10.66	11.12	11.59	12.05	12.51	12.98	13.44	13.90	14.37	14.83	15.29	15.76	16.22	16.69	17.15	17.61	18.07	18.54
34	10.55	11.05	11.56	12.06	12.56	13.06	13.57	14.07	14.57	15.07	15.57	16.08	16.58	17.08	17.59	18.09	18.59	19.09	19.59	20.10
35	11.43	11.97	12.51	13.06	13.60	14.15	14.69	15.23	15.78	16.32	16.87	17.41	17.95	18.50	19.04	19.59	20.13	20.67	21.22	21.76
36	12.36	12.95	13.54	14.13	14.72	15.31	15.89	16.48	17.07	17.66	18.25	18.84	19.43	20.01	20.60	21.19	21.78	22.37	22.96	23.55
37	13.36	14.00	14.64	15.27	15.91	16.55	17.19	17.82	18.46	19.09	19.73	20.36	21.00	21.64	22.27	22.91	23.55	24.18	24.82	25.46
38	14.44	15.13	15.81	16.50	17.19	17.88	18.56	19.25	19.94	20.63	21.31	22.00	22.69	23.38	24.06	24.75	25.44	26.13	26.81	27.50
39	15.59	16.33	17.07	17.82	18.56	19.30	20.04	20.78	21.53	22.27	23.01	23.75	24.50	25.24	25.98	26.72	27.47	28.21	28.95	29.69
40	16.82	17.62	18.42	19.23	20.03	20.83	21.63	22.43	23.23	24.03	24.83	25.63	26.43	27.24	28.04	28.84	29.64	30.44	31.24	32.04
41	18.15	19.01	19.87	20.74	21.60	22.47	23.33	24.19	25.06	25.92	26.79	27.65	28.51	29.38	30.24	31.11	31.97	32.83	33.70	34.56
42	19.57	20.50	21.43	22.36	23.29	24.22	25.16	26.09	27.02	27.95	28.88	29.82	30.75	31.68	32.61	33.54	34.47	35.41	36.34	37.27
43	21.09	22.10	23.10	24.11	25.11	26.11	27.12	28.12	29.13	30.13	31.14	32.14	33.15	34.15	35.15	36.16	37.16	38.17	39.17	40.18
44	22.73	23.82	24.90	25.98	27.06	28.15	29.23	30.31	31.39	32.48	33.56	34.64	35.72	36.81	37.89	38.97	40.05	41.14	42.22	43.30
45	24.50	25.67	26.83	28.00	29.17	30.33	31.50	32.67	33.83	35.00	36.17	37.33	38.50	39.67	40.83	42.00	43.17	44.33	45.50	46.67
46	26.40	27.66	28.92	30.17	31.43	32.69	33.95	35.20	36.46	37.72	38.98	40.23	41.49	42.75	44.00	45.26	46.52	47.78	49.03	50.29
47	28.46	29.81	31.17	32.52	33.88	35.23	36.59	37.94	39.30	40.65	42.01	43.36	44.72	46.07	47.43	48.78	50.14	51.49	52.85	54.20
48	30.67	32.13	33.59	35.05	36.51	37.97	39.43	40.89	42.36	43.82	45.28	46.74	48.20	49.66	51.12	52.58	54.04	55.50	56.96	58.42
49	33.07	34.64	36.22	37.79	39.37	40.94	42.51	44.09	45.66	47.24	48.81	50.39	51.96	53.54	55.11	56.69	58.26	59.83	61.41	62.98
50	35.66	37.36	39.06	40.75	42.45	44.15	45.85	47.55	49.24	50.94	52.64	54.34	56.04	57.74	59.43	61.13	62.83	64.53	66.23	67.92
51	38.47	40.30	42.14	43.97	45.80	47.63	49.46	51.30	53.13	54.96	56.79	58.62	60.46	62.29	64.12	65.95	67.78	69.62	71.45	73.28
52	41.52	43.50	45.48	47.46	49.43	51.41	53.39	55.37	57.34	59.32	61.30	63.28	65.25	67.23	69.21	71.19	73.16	75.14	77.12	79.09
53	44.84	46.98	49.12	51.25	53.39	55.52	57.66	59.79	61.93	64.06	66.20	68.33	70.47	72.61	74.74	76.88	79.01	81.15	83.28	85.42
54	48.46	50.77	53.08	55.38	57.69	60.00	62.31	64.62	66.92	69.23	71.54	73.85	76.16	78.46	80.77	83.08	85.39	87.69	90.00	92.31
55	52.41	54.91	57.40	59.90	62.40	64.89	67.39	69.88	72.38	74.87	77.37	79.87	82.36	84.86	87.35	89.85	92.34	94.84	97.34	99.83
56	56.73	59.43	62.14	64.84	67.54	70.24	72.94	75.64	78.34	81.05	83.75	86.45	89.15	91.85	94.55	97.25	99.96	102.66	105.36	108.06
57	61.47	64.40	67.32	70.25	73.18	76.11	79.03	81.96	84.89	87.81	90.74	93.67	96.60	99.52	102.45	105.38	108.30	111.23	114.16	117.09
58	66.68	69.85	73.03	76.20	79.38	82.55	85.73	88.90	92.08	95.25	98.43	101.60	104.78	107.95	111.13	114.30	117.48	120.65	123.83	127.00
59	72.41	75.86	79.31	82.76	86.20	89.65	93.10	96.55	100.00	103.45	106.89	110.34	113.79	117.24	120.69	124.13	127.58	131.03	134.48	137.93
60	78.75	82.50	86.25	90.00	93.75	97.50	101.25	105.00	108.75	112.50	116.25	120.00	123.75	127.50	131.25	135.00	138.75	142.50	146.25	150.00